Asian Journal of Chemistry; Vol. 26, No. 5 (2014), 1358-1362

ASIAN JOURNAL OF CHEMISTRY

http://dx.doi.org/10.14233/ajchem.2014.17231

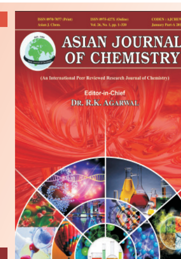

Design of Low-Energy Modest-Resolution (sub-50 nm) Microcolumn Easy to Fabricate†

TAE-SIK OH[1], SEUNGJOON AHN[1], DAE-WOOK KIM[1], SEONG JOON AHN[2] and HO SEOB KIM[1,*]

[1]Department of Information Display, Sun Moon University, Asan, Chungnam, Republic of Korea
[2]Department of I & C Engineering, Sun Moon University, Asan, Chungnam, Republic of Korea

*Corresponding author: Fax: +82 41 5302260; E-mail: hskim3@sunmoon.ac.kr

Published online: 1 March 2014; AJC-14772

The electrodes of the electron optical microcolumn are precisely fabricated using the micro-electro-mechanical systems technology, which makes it possible to minimize the electron beam size as well as the optical aberrations compared with those of the conventional electron columns. It is, however, necessary to make the apertures of the electrodes very small to obtain high resolution and it takes lots of time and effort to align the apertures of the electrodes. In this work, we have designed a new structure of electron optical microcolumn in which the apertures of the electrodes are relatively large, so the alignment is very easy to carry out while maintaining the modest resolving power (sub 50-nm).

Keywords: Microcolumn, Auxiliary control electrode, Electron beam size, Sub-50 nm resolution.

INTRODUCTION

Since the first microcolumn was developed in IBM in T.J. Watson Laboratory in early 1990s, there have been steady research and improvement made in the device. Basically the microcolumn is an ultra-small electron column which has very simple structure with total length of about 10 mm (Fig. 1). Due to the short length of the microcolumn, the scattering between electrons within the column can be minimized. In addition, the high-quality electrodes reduce the optical aberration, which leads to the enhanced performance of the electron columns. To obtain the quality electrodes, precise machining of the very small holes with aperture of several μm is required and these days the micro-electro-mechanical system (MEMS) technologies are used for the machining[1-3]. One of the most promising advantages of the microcolumn is that the small multiple electron beam (e-beam) sources might be possibly constructed using many microcolumns, which today's semiconductor and display industries need in order to overcome the low throughput of the e-beam equipment being used in the lithography and inspection or critical dimension (CD) measurement of the semiconductor devices[4-10].

Fig. 1 is the typical structure of the microcolumn composed of electron emitter (or tip-emitter), source lens, deflector and focus lens (or Einzel lens), among which the source lens is a very important component determining the electrical characteristic of the microcolumn by inducing the emission of the e-beam and controlling its trajectory. The source lens is composed of three electrodes called the extractor, the accelerator and the limiter each of which induces the emission of electrons from the tip-emitter, accelerates the electrons and controls the size of the e-beam, respectively. The electric fields formed across the source lens, or equivalently the biases applied to the electrodes, determine the behaviour of the e-beam.

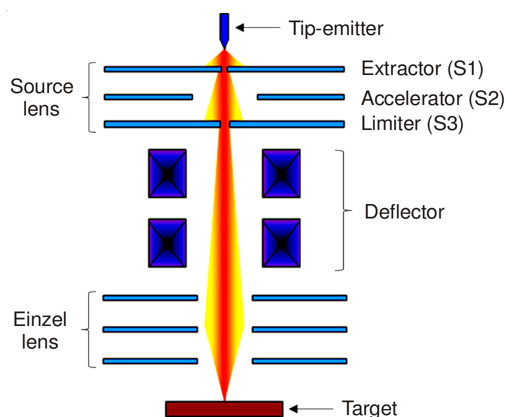

Fig. 1. Structure of the microcolumn developed by the IBM in T.J. Watson Laboratory

†Presented at The 7th International Conference on Multi-functional Materials and Applications, held on 22-24 November 2013, Anhui University of Science & Technology, Huainan, Anhui Province, P.R. China

Based on the simple design shown in Fig. 1, several low-energy (about 1 keV) microcolumns have been developed whose e-beam currents were higher than 1 nA and resolutions were ranging from 10-40 nm[11-13]. But, to achieve such high resolutions, the apertures of the extractor and limiter have to be as small as 5.0 and 2.5 μm, respectively, which makes the alignment between the tip-emitter and the source lens so difficult that high-precision positioner like the STM-scanner is required for the alignment. Therefore it takes lots of time and efforts to manufacture the microcolumn.

In this work, to resolve such a problem, we have designed a low-energy modest-resolution (sub-50 nm) microcolumn using the commercial simulator Opera (ver. 15) where the apertures of the electrodes are large enough that there is little difficulty in the alignment. To suppress excessive degradation of the resolution caused by large apertures, we have inserted an auxiliary control electrode between the extractor and the accelerator and optimized the geometrical and electrical parameters.

EXPERIMENTAL

Verification of the reliability of the design tool: Before we proceed to design the microcolumn, it is necessary and meaningful to check the validity of our 3D-simulation tool Opera (ver. 15) by comparing the published simulation and experimental data with those of our simulation. In this work, we used the microcolumn developed by the IBM group as the reference[12]. Fig. 2 shows the equipotential lines near the electron lenses and the e-beam trajectory produced by the simulator Opera for the reference microcolumn. The details of the internal structure (which will be called IR-5 model afterwards) and operational condition is given in Table-1, where S1, S2 and S3 stand for the extractor, the accelerator and the limiter, respectively.

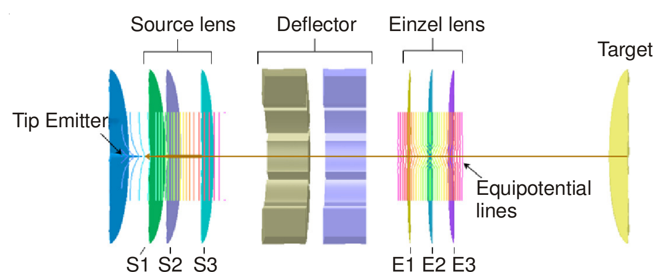

Fig. 2. Equipotential lines near the electron lenses and the e-beam trajectory produced by Opera simulator

Fig. 3 is the simulated behaviour of the e-beam diameters when the distance between the tip and the extractor varied as 50, 70 and 100 μm. The voltage biases applied to the tip-emitter, S1 (the extractor), S2 (the accelerator), S3 (the limiter) were 1 keV, -700 V (variable), 0 V and 0 V, respectively. The bias -700 V to the S1 was set to make the e-beam current from the tip-emitter be 10 μA that was the experimental condition of the IBM group[12,13]. The distance between the Einzel lens and the target which is called the working distance was 2 mm. In the graph, the value of the diameter at 10 % current density means the average diameter of the e-beam cross-section at the target surface which was formed by connecting the points at which the local current density was 10 % of the maximum current density around the center of Gaussian beam profile. The beam spot size is defined as the beam diameter at 50 % current density that is represented by FWHM (full width at half-maximum) line in the figure.

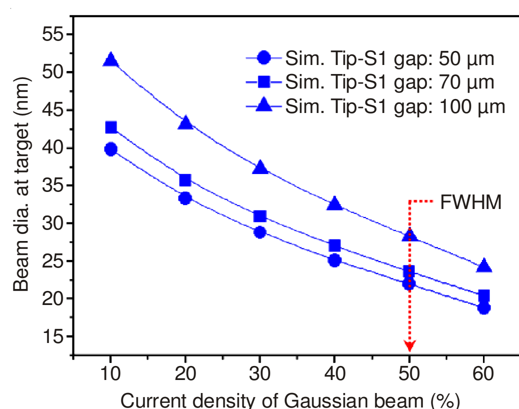

Fig. 3. Diameter of the e-beam in the target surface as the distance between the tip and extractor varies

The simulated results of Fig. 3 are consistent with those of the IBM group. For example, when the distance between the tip and S1 was 50 μm, the simulated beam spot size was 22 nm while the reported value of the IBM group was 23 nm. The consistency confirms that the 3D simulator Opera gives reliable data and can be used as a powerful design tool for the microcolumns. In the next section, we present the detailed procedure on the design of modest-resolution microcolumn using the Opera simulator.

Design of modest-resolution microcolumn with large lens' apertures: In the previous section, the aperture sizes or diameters of the extractor (S1) and the limiter (S3) were as small as 5.0 and 2.5 μm, respectively. As the apertures are getting smaller, so is the spot size of the e-beam and the resolution of the microcolumn is getting higher. But such small apertures not only make the alignment of the components of the microcolumn difficult but also reduce the e-beam current significantly. Therefore it is important to optimize the aperture sizes according to the applications which the microcolumn is used for.

In this work, we tried to design the microcolumn the resolution of which is adequate for the inspections of the semiconductor and display devices with relatively large apertures of the extractor (S1) and limiter (S3) for the easy alignment of the source lens. The large aperture of the extractor especially makes the alignment of the emitter-tip and the extractor easy

TABLE-1
DIMENSION AND DRIVING VOLTAGE OF TIP AND ELECTRODES IN THE IR-5 MODEL

	Tip	S1	S2	S3	Tip-S1	S1-S2	S2-S3
Diameter/gap (μm)	Φ0.1	Φ5	Φ100	Φ2.5	50-100	200	400
Driving voltage (V)	-1000	-700	0	0	–	–	–

while the enlarged aperture of the limiter primarily contributes to increasing the e-beam current that arrives to the target. Thus the enlargement of the apertures is good for the enhancement of the e-beam quality as well as the fabrication of the micro-column.

But, as a negative effect of the large apertures, the resolution of the microcolumn becomes necessarily degraded, which has been alleviated by an auxiliary control electrode inserted between the extractor (S1) and the accelerator (S2). Fig. 4 is the newly-designed microcolumn where the auxiliary control electrode is denoted by S2s whose physical and electrical parameters are shown in Table-2. The structure shown in Fig. 4 will be called as ND-50 model now. The auxiliary control electrode (S2s) re-converges the diverging e-beam emerging from the extractor (S1) and eventually controls the electron trajectory to transfer the optimized e-beam to the Einzel lens.

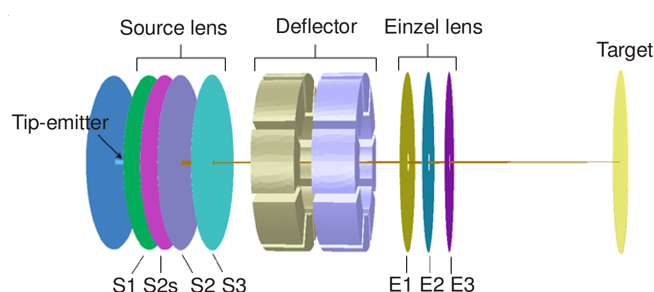

Fig. 4. Structure of the modest-resolution microcolumn with modified design of the source lens (ND-50 model) where an auxiliary control electrode (S2s) is added

For the ND-50 model, we have investigated various characteristics using the Opera whose validity was confirmed in the previous section. First, we estimated the effect of the S2s electrode of our ND-50 model, for which we compare the results with those of other two configurations. One has the same configuration with ND-50 model except there is no S2s electrode and is named as ND-50N model. The other is called IR-5-10 model whose structure is same with that of IR-5 model but the diameter of S3 aperture is set to be 10 µm which is identical with other models so that the comparison makes sense.

Fig. 5 shows the beam diameter characteristic of the three models. The bias voltages to the tip-emitter and S3 were -1000 and 0 V, respectively for all the models. For IR-5-10 and ND-50N models, the bias to the S1 and S2 were 700 V and -800 V. To make the similar operating environment, the biases to S1, S2s and S2 for ND-50 model were set to be 697.5 V, -800 and 0 V, respectively. Under these conditions, the e-beam currents from the emitter-tip were also turned out to be 10 µA. The working distance was 2.0 mm. As observed in Fig. 5(a), the beam diameter of ND-50 model is much smaller than those of ND-50N and IR-5-10 models, which clearly shows that the auxiliary control electrode S2s works excellently to reduce the beam diameter and hence improves the resolution of the

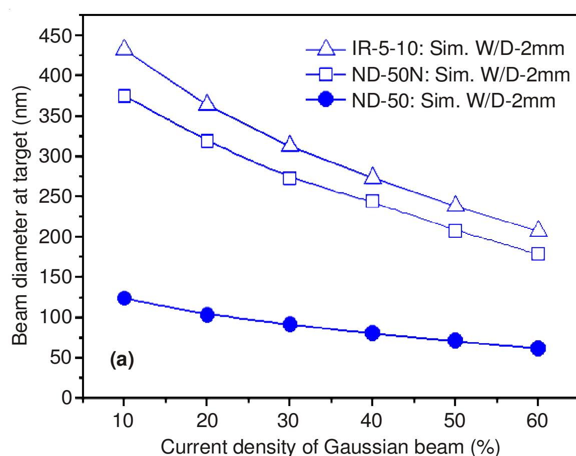

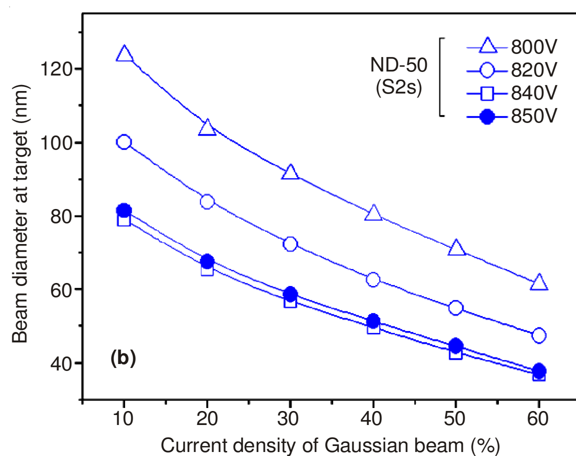

Fig. 5. (a) Characteristics of the beam diameter of ND-50, ND-50N and IR-5-10 model. (b) Behaviour of the beam diameter according to the various bias of the S2s electrode in the ND-50 model

microcolumn. The effect of the S2s in the ND-50 model can be confirmed more in Fig. 5(b) where the beam diameter is getting decreased as the magnitude of the bias increases.

In Fig. 6, we have calculated the e-beam currents emerging from the tip-emitter (the tip currents) and the e-beam currents reaching the target (the probe currents) when the bias to the S2s electrode varied from -800 to -860 V. The simulation was carried out with respect to the two different sizes of the S3 aperture, that is, 2.5 and 10 µm. As we can expect, the tip currents (denoted by the open triangles and circles) are not affected much by the S2s bias regardless of the aperture size of S3. For the probe currents (solid triangles and circles in the figure), the dependence on the S2s bias is hardly noticeable when the aperture size of S3 is 2.5 µm. It seems that for such a small limiting aperture, most of electrons except those passing straightly through the aperture are removed by the limiter; hence the control of the e-beam trajectory does not make any change to the probe current. On the contrary, when the aperture is as sufficiently large as 10 µm, the probe current increases more than two times as the bias varies from -800 to -860 V.

TABLE-2
DIMENSION AND DRIVING VOLTAGE OF TIP AND ELECTRODES IN THE ND-50 MODEL

	Tip	S1	S2s	S2	S3	Tip-S1	S1-S2s	S2s-S2	S2-S3
Diameter/gap (µm)	Φ0.1	Φ50	Φ50	Φ50	Φ10	50	200	200	400
Driving voltage (V)	-1000	-697.5	Variable	0	0	–	–	–	–

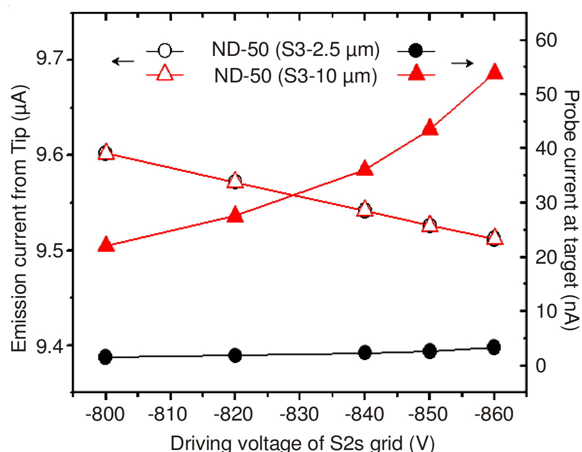

Fig. 6. e-beam currents emerging from the tip (the tip currents) and at the target (the probe currents) versus the bias to the S2s electrode with respect to the two different sizes of the S3 aperture

Combining the results of Figs. 5 and 6, we may well expect that we can obtain high probe current with large aperture of S3 while keeping the small beam spot size, for the increase of the S2s bias results in the increase of the probe current and reduction of the e-beam size.

As observed in Fig. 7, however, there is a limit in the S2s bias within which the increase of the bias voltage leads to better result. For both of the working distances (W/D) of 1 and 2 mm, the probe beam currents (denoted by the solid triangles and squares) are increasing according to the magnitude of the S2s bias. But when the bias voltage exceeds -850 V, the beam spot size (denoted by the half-filled triangles and squares in the figure) at the target changes its tendency and begins to increase rapidly. This phenomena can be explained by the over focusing of the e-beam inside the source lens when the bias of the S2s electrode is higher than -850 V. The over-focused e-beam begins to diverge again before it enters the Einzel lens, which is called the crossover and the divergence is too strong to be effectively controlled in the Einzel lens. Hence once the crossover takes place, the beam spot size grows rapidly as the working distance increases as shown in Fig. 7.

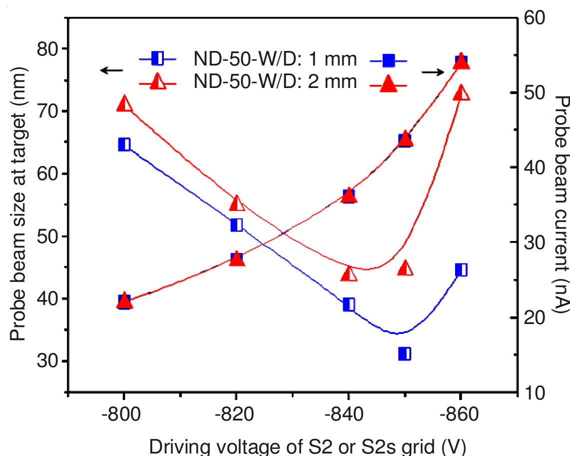

Fig. 7. Magnitude and size of the probe beam *versus* the bias voltages of the auxiliary control electrode (S2s)

Based on the knowledge obtained from Figs. 5-7, we have optimized several parameters of the ND-50 model and simulated its beam diameters for the working distances of 1 and 2 mm. To check the gap between the simulation and reality, we have also carried out the same simulation with respect to the IR-5 model and compared it with the experimentally measured data[12].

In Fig. 8, the open circles and open squares represent the simulated beam diameters for the IR-5 model when the working distance was 1 and 2 mm, respectively. As observed, the simulated beam spot sizes, that are the beam diameters of current density of 50 %, are 16 and 22 nm for the working distance of 1 and 2 mm, respectively. Experimentally measured beam diameters for the IR-5 model were 18.5 and 30 nm, which are denoted by the solid stars in the figure. Since the value 18.5 nm corresponds to the simulated beam diameter at current density of 40 %, it may presume that for working distance of 1 mm, the discrepancy between the simulated value and the real one can be compensated by 10 % shift along the horizontal axis. In the similar way, for working distance of 2 mm, the real beam spot size can be obtained at the current density of 30 % rather than at 50 %.

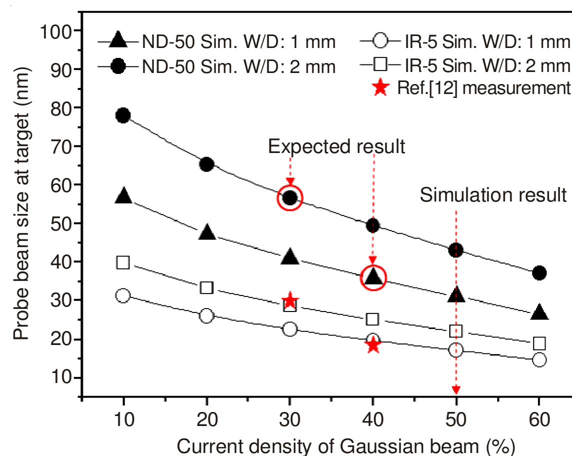

Fig. 8. Expected experimental beam diameter according to the various current density of Gaussian beam in the IR-5 and ND-50 model

The solid triangles and circles in Fig. 8 are the simulated beam diameters in the ND-50 model for the working distances of 1 and 2 mm, respectively. According to the same logic, we have estimated the real beam spot sizes from the simulated values for the ND-50 model. For the working distance of 1 mm, the simulated beam spot size is 31.1 nm and the real beam spot size is estimated to be 35.7 nm which is the simulated beam diameter at current density of 40 %. For the working distance of 2 mm, the real beam spot size is estimated to be 56.6 nm which is the simulated beam diameter at current density of 30 %.

Conclusion

We have designed a low-energy modest-resolution microcolumn that can be used for inspecting the semiconductor and display devices using the 3D simulator Opera. To overcome the problems caused by small apertures of the extractor and the limiter in the source lens, we have enlarged the apertures while inserting the auxiliary control electrode between the extractor and the accelerator in order to prevent the excessive degradation of the resolution caused by the large apertures.

The newly designed microcolumn is expected to be easy to fabricate since it has little difficulty in aligning the source lens with the tip-emitter. In addition, the probe beam current is estimated to be higher than 10 nA, which is much higher than that of the previous microcolumns reported and sufficient for most inspections.

The validity of the simulation has been confirmed by the comparison with the previous research and through the appropriate calibration, we have extracted the real beam spot size from the simulated data on the beam diameters. In the optimized microcolumn, the diameters of the extractor and limiter were 50 μm and 10 μm, respectively. The bias to the auxiliary control electrode was -850 V. For the working distance of 1 mm, the beam spot size has been estimated to be 35.7 nm, which satisfies the criteria of sub-50-nm resolution very well. It is expected from present research contribute to realize the microcolumn that is easy to fabricate and useful for the inspection applications.

ACKNOWLEDGEMENTS

This work was supported by the IT R&D program of MKE/KEIT. [10039226, Development of Actinic EUV mask inspection tool and multiple electron wafer inspection technology].

REFERENCES

1. L.P. Muray, U. Staufer, D. Kern and T.H.P. Chang, *J. Vac. Sci. Technol. B*, **10**, 2749 (1992).
2. A. Singh, R. Mukherjee, K. Turner and S. Shaw, *J. Sound Vibrat*., **286**, 637 (2005).
3. C. DaVia, J. Hasi, C. Kenney, A. Kok and S. Parker, *Nucl. Instrum. Methods Phys. Res. A*, **549**, 122 (2005).
4. T.H.P. Chang, M.G.R. Thomson, E. Kratschmer, H.S. Kim, M.L. Yu, K.Y. Lee, S.A. Rishton, B.W. Hussey and S. Zolgharnain, *J. Vac. Sci. Technol. B*, **14**, 3774 (1996).
5. L.P. Muray, K.Y. Lee, J.P. Spallas, M. Mankos, Y. Hsu, M.R. Gmur, H.S. Gross, C.B. Stebler and T.H.P. Chang, *Microelectron. Eng*., **53**, 271 (2000).
6. T.H.P. Chang, M. Mankos, K.Y. Lee and L.P. Muray, *Microelectron. Eng*., **57-58**, 117 (2001).
7. Y.C. Kim, D.W. Kim, S. Ahn, T.S. Oh, J.B. Kim, Y.S. Roh, D.G. Hasko and H.S. Kim, *J. Vac. Sci. Technol. A*, **27**, 3208 (2009).
8. C.D. Bubeck, A. Fleischmann, G. Knell, R.Y. Lutsch, E. Plies and D. Winkler, *Nucl. Instrum. Methods Phys. Res. A*, **427**, 104 (1999).
9. H.S. Kim, D.W. Kim, S.J. Ahn, Y.C. Kim, S.S. Park, K.W. Park, N.W. Hwang, S.W. Jin and S.Y. Bae, *Microelectron. Eng*., **85**, 782 (2008).
10. T.S. Oh, D.W. Kim, Y.C. Kim, S.J. Ahn, G.H. Lee and H.S. Kim, *J. Vac. Sci. Technol*., **28**, C6C69 (2010).
11. E. Kratschmer, H.S. Kim, M.G.R. Thomson, K.Y. Lee, S.A. Rishton, M.L. Yu and T.H.P. Chang, *J. Vac. Sci. Technol. B*, **12**, 3503 (1994).
12. E. Kratschmer, H.S. Kim, M.G.R. Thomson, K.Y. Lee, S.A. Rishton, M.L. Yu and T.H.P. Chang, *J. Vac. Sci. Technol. B*, **13**, 2498 (1995).
13. E. Kratschmer, *J. Vac. Sci. Technol. B*, **14**, 3792 (1996).